Journal of Sol-Gel Science and Technology (2023) 107:218–226
https://doi.org/10.1007/s10971-022-05978-8

INVITED PAPER: FUNDAMENTALS OF SOL-GEL AND HYBRID MATERIALS PROCESSING

Influence of drying technique on Pt/In_2O_3 aerogels for methanol steam reforming

Lukas Thoni[1] · Nadia Metzkow[1] · Alexander Eychmüller[1]

Received: 17 August 2022 / Accepted: 19 October 2022 / Published online: 11 November 2022

Abstract

In this paper we present a comparison of aerogels which are dried under different conditions. Of those, most important are the solvent, temperature, and pressure. Criteria of comparison rely mostly on results from analysis of nitrogen adsorption experiments, as well as transmission electron microscopy imaging. Platinum loaded indium oxide aerogels were picked as a model system for this study as they can be used as highly effective heterogeneous catalysts in methanol steam reforming. The compared drying methods include supercritical drying from CO_2, supercritical CO_2 - ethanol mixture, freeze drying from tert-butanol and ambient conditions drying from acetone and 1-Methoxyheptafluoropropane. High porosities and large specific surface areas can be achieved via supercritical, freeze- and ambient conditions drying, while retaining the original gel morphology in this system for most methods except freeze drying and ambient conditions drying from acetone.

Graphical abstract

Schematic of a phase diagram (left) describing drying methods for solvogels by sublimation, evaporation or supercritical drying of the solvent. The results of those methods on the final aerogels are compared for the system of indium oxide aerogels loaded with platinum nanoparticles.

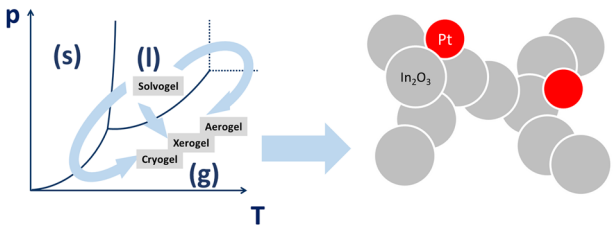

Keywords Aerogel · Xerogel · Cryogel · Catalyst · BET Analysis · Specific Surface Area

Highlights

- Supercritical drying and ambient conditions drying can yield gels with similar surface, pore and morphological properties.
- The results of drying gels under ambient conditions are mainly depending on the solvent choice.
- Freeze drying and ambient conditions drying affect the gel structure the most for platinum on indium oxide gels.

Supplementary information The online version contains supplementary material available at https://doi.org/10.1007/s10971-022-05978-8.

✉ Alexander Eychmüller
Alexander.eychmueller@tu-dresden.de

[1] Institute of Physical Chemistry, TU Dresden, 01062 Dresden, Germany

- The aerogel system of Pt/In_2O_3 has been reported to have an activity of 800 mol (H_2)/(mol (Pt)× h) with a CO_2 selectivity of 99.5% at 300 °C in the methanol steam reforming process. These are unprecedented values for methanol steam reforming catalysts in this temperature regime.

1 Introduction

Aerogels are mostly known for their high porosity, and large specific surface areas, consisting of mainly air surrounded by a solid gel network. Silica aerogels have since made themselves a name as excellent thermal insulators since their discovery in the 1930s [1]. The large surface area can also be of use in other areas such as sensors, electrocatalysis, or more generally heterogeneous catalysis [2–4]. Provided by the nanostructured macroscopic body of the aerogels a major factor contributing to the use in heterogeneous catalysis is the enlargement of surface area in aerogels respective to their bulk counterparts [5].

Aerogels are not limited to silica, the word is describing a class of materials which can be represented by different elements or compounds [6]. Most aerogels are created by the sol–gel method. One advantage of this method rests in the homogeneous nature of coming from an evenly dissolved precursor to the formation of a three-dimensional network of interconnected nanoparticles in solution. Here, we use an epoxide assisted gelation protocol introduced by Gash and Tillotson to create indium hydroxide gels which are loaded with platinum nanoparticles during synthesis [7]. The approach to include the loading during gel formation compared to deposition methods yields a more homogeneous distribution of platinum throughout the gel network, an important factor in catalyst preparation. The homogeneity of loading an oxidic gel network with other metal nanoparticles by a sol–gel process can also be found in various other systems [6, 8]. In this specific presented case, indium oxide acts as a support material as well as interacting player with platinum. During the catalyst preparation an intermetallic phase is formed, which in combination with the indium oxide is one of the most active and selective catalyst systems for methanol steam reforming known to date [9, 10]. This success stems also partly from the homogeneity of the sol–gel method, the nanoscale nature of the compounds and a resulting large cross sectional area of the two active components. A full catalytic study of the Pt/In_2O_3 aerogel system, which is the topic of this publication, including thermal and reductive activation of the aerogel catalyst can be found in our previous publication by Köwitsch et al. [9]. One major drawback to working in a gelation solution is the presence of a solvent in the gels` pores. The liquid phase has to be removed carefully as not to destroy the often fragile gel network by capillary forces during evaporation, which can happen when drying at standard conditions [11]. A newer approach to drying under ambient pressure relies on the so called "springback" effect of the gel network, when drying at elevated temperatures [12]. Traditionally, aerogels are prepared by supercritical drying either directly from the reaction solution, alcohols or liquid CO_2. The latter is most often used as it yields reproducible results and a low danger of the process itself, regarding operating pressure and temperature. Another procedure used in large scale also in the food industry is freeze drying. The solvent is frozen and then sublimated by a vacuum.

When looking at a standard phase diagram, during drying generally crossing of the liquid-gas phase boundary is avoided by moving around the critical or the triple point (Fig. 1).

The dilemma in aerogel production is that the controlled solvent removal is one step in aerogel production that consumes a lot of energy and at the same time it is unavoidable to achieve aerogels at all. Either by choosing an apparatus or solvents that are needed to reach drying conditions, in any case energy is needed to make the solvent gaseous, from where it dissipates into the environment. With the drying step being of such high importance in aerogel production a scientific comparison of the resulting gels shall be done here on the case of platinum loaded indium hydroxide gels. The importance of the drying technique has made its way into the nomenclature of the resulting gels. Supercritically dried gels are generally called

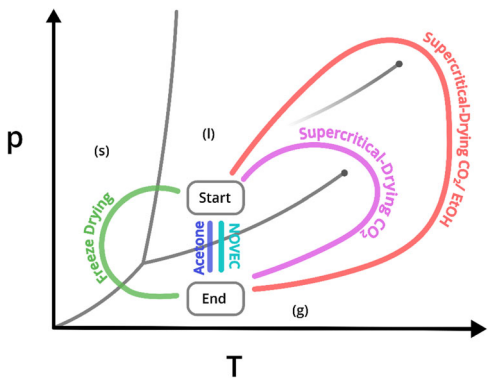

Fig. 1 Phase diagram scheme to visualize the difference in the drying techniques. The phase start and endpoint describes the medium which fills the pores. Beginning with the solvogel, and pores filled with solvent, the system can either be driven via the critical point, via the solid state of the solvent and sublimation or just directly crossing the liquid-gas phase boundary with ambient conditions drying. The values are not accurate as it is difficult to include the phase diagrams of several different solvents as well as two component systems represented by the SCEC method

Table 1 Sample processing and drying conditions of each of the five chosen methods

Reference	SCC	SCEC	FD	ACA	ACN
Drying process	Supercritical CO_2	Supercritical CO_2/ EtOH mixture	Freeze Drying	Ambient conditions drying	Ambient conditions drying
Solvent exchange (number of times)	EtOH (6) CO_2 (6-7)	EtOH (6) Sc-CO_2/ EtOH (6-7)	EtOH (6) t-BuOH (6)	EtOH (6) Acetone (6)	EtOH (6) NOVEC (6)
Drying solvent	CO_2	CO_2/EtOH	t-BuOH	Acetone	NOVEC
Temperature	37 °C	60 °C	−80 °C	25 °C	25 °C
Pressure	80 bar	110 bar	10^{-4} bar	1012 bar	1012 bar
Drying time	24 h (time in autoclave)	2 h	24 h	48 h	48 h

NOVEC-7000 represents the solvent of 1-Methoxyheptafluoropropane

aerogels (greek aero = air), freeze-dried gels are cryogels (greek cryo = cold) and under ambient conditions dried gels are xerogels (greek xero = dry) [13–15]. The first of those is the typical method of aerogel production and most widespread. For this work, disregarding how gels are dried they still are comparable in their nature and shall thus all be referred to as aerogels. To distinguish between samples, it will be referred to their drying method (Table 1). Aerogels shall be compared regarding their surface, pores, morphology and crystallinity.

2 Experimental

The process of gelation follows the same recipe for all of the discussed gels. 10 mL of a 0,25 M indium chloride (Alfa Aesar, 99.999%) solution in ethanol (Berkel AHK, 99%, 1% petrol ether) are stirred at room temperature. 2475 mL deionized water is added to allow the metal precursor to hydrate also allowing the hydrolysis of the epoxide later on and the solution is stirred for 5 min. Then, 5 mL of propylene oxide (Sigma-Aldrich, 99%) are added to initiate the gelation. After 2 min, 890 µL of a 0,2 M solution of platinum (IV) chloride (Sigma-Aldrich, 99.999%) in ethanol is added to the reaction mix and stirred for 30 s. Then, the platinum in the gelation solution is reduced by addition of a freshly prepared solution of 10 mg sodium borohydride (Sigma-Aldrich, 99.99%) in 2 mL water. This yields gels with a 10 weight-% loading of platinum on indium oxide. The otherwise clear solution immediately turns black upon the formation of platinum nanoparticles. Gel formation occurs within 20 min after addition of the epoxide. The solvogels are then left undisturbed over night for aging. Subsequently, all the gels are washed six times over three days with ethanol to remove byproducts of the gelation such as salts and unwanted solvent residues. Gels are then prepared and dried under the given conditions and from each named solvent (Table 1).

For the drying techniques there shall be compared five different systems based on four different methods. Firstly, supercritical drying after the Tewari method [16]. Here a solvogel in ethanol is put in an autoclave where there is a solvent exchange at low temperature from ethanol to CO_2. Then, the pure CO_2 is turned supercritical by adjusting pressure and temperature and finally removed, so that only a gas is left in the pores. The second supercritical drying method relies on a supercritical mixture of ethanol and CO_2 after Bommel et al. [17, 18]. Sufficiently high pressure and temperature are chosen, so that the mixture of ethanol in the gel pores and injected CO_2 reaches the supercritical state immediately after filling the autoclave. To reach the supercritical state of the mixture higher temperature and pressure is required than for the single component pure CO_2 system. The sample is then kept under supercritical conditions, where solvent exchange happens. After completion, CO_2 is removed and remains in gaseous form in the pores. When using freeze-drying there is first a solvent exchange to tert-butanol (ACROS 99,5%), a solvent with conveniently low sublimation point. The samples are then frozen in liquid nitrogen and put in a freeze dry device, which keeps the samples at 10^{-4} mbar and 193 K. Upon insertion, tert-butanol instantly starts to sublimate, and is removed without putting the gel network under capillary forces stress. Though not viable for this specific system, another readily available solvent for freeze drying is water. Samples dried under ambient conditions are left in a Petri dish in the fume hood for two days, where the solvents can evaporate under room temperature and ambient pressure. The solvents chosen here are Acetone (MERCK, puriss 99,5%) and NOVEC 7000 (1-Methoxyheptafluoropropane, Sigma Aldrich, 99,5%) the use of the latter is based on a patent from Steiner et al. [19].

The nitrogen physisorption experiments are conducted on a NOVA 3000e device after being activated for 3 h at

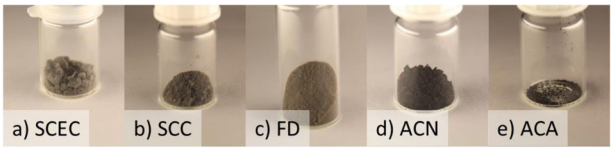

Fig. 2 Pictures of the individual gel samples for the (**a**) SCEC, (**b**) SCC, (**c**) FD, (**d**) CAN, and (**e**) ACA methods show voluminous gels for all drying methods except ambient conditions drying from acetone. Here a strong shrinkage can be seen macroscopically. All wet gel monoliths crumble during solvent exchange due to shrinkage, which results in aerogel powders

110 °C. Analysis of the isotherms is conducted with the NOVAWIN Software using the BET (Brunauer-Emmett-Teller) method. For transmission electron microscopy samples are dispersed in ethanol, ultrasonicated for 10 s and added dropwise on a standard sample grid. The shown images are recorded on a LIBRA 120 from ZEISS. Thermogravimetry analysis is conducted in the device TGA/DSC 1 STARe from METTLER TOLEDO. Samples are first heated up to 300 °C with a ramp of 10 K min^{-1} and then kept at this temperature for 30 min, all under air. Powder X-ray diffractograms are measured on the device D2 Phaser from BRUKER in the 2 θ range from 10° to 80° with Cu K_α source. For this, dispersed samples are dropcast on a silicium wafer sample holder.

3 Results and discussion

To give an overview of the obtained dried gels images are shown in Fig. 2. The wet gel monoliths from synthesis experience strain from shrinking and/or swelling during the solvent exchange and have the macroscopic morphology of light powders. Pure indium hydroxide is white with the platinum loading introducing a dark gray shade. The ACA method yields as the only drying technique strongly shrunken, dense particles which are in a darker shade than the other samples due to the higher concentration of platinum nanoparticles per volume of dried gels. This effect can be seen as well for the ACN aerogels, which undergo a slight macroscopic shrinkage during drying but still retain their porosity and surface area as will be explained by the nitrogen adsorption experiments. These macroscopic observations are as well reflected in the transmission electron microscopy images and measured web thickness (Fig. 3, Supplementary Fig. 1).

For the first technique a slight shrinkage can be observed during the drying process, surprisingly this does not seem to affect either specific surface area, total pore volume or morphology. The biggest impact of drying can be observed under ambient conditions from acetone. The pore collapse due to capillary forces of the solvent on the gel matrix leads to a dense morphology, in which the original gel structure

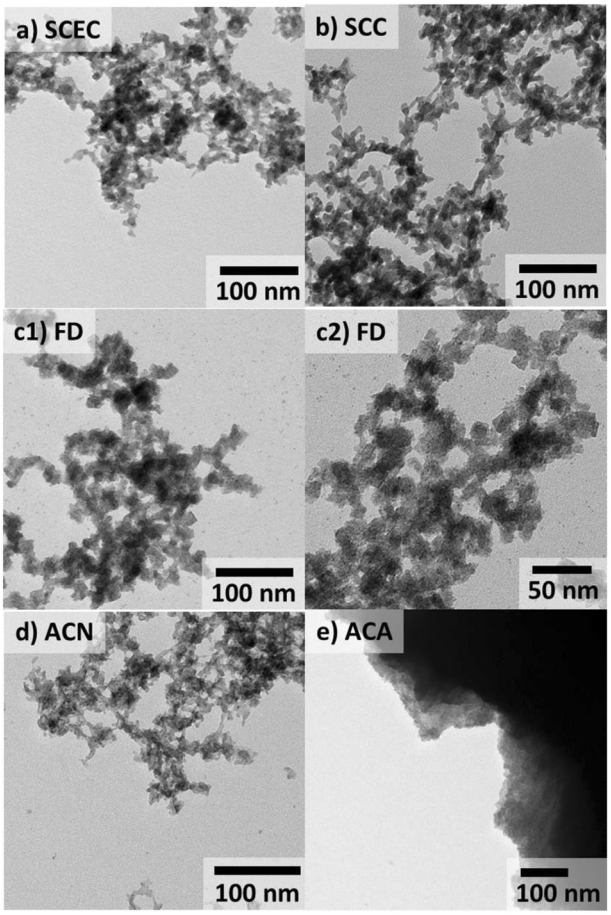

Fig. 3 TEM pictures of the as-prepared aerogel samples. TEM images comparing the methods of (**a**) SCEC, (**b**) SCC, (**c**) FD, (**d**) CAN, and (**e**) ACA. c2) shows a higher magnification image of the freeze-dried gels highlighting the presence of nanoparticles detached from the gel network

cannot be observed anymore. The significant shrinkage affects the SSA and total pore volume strongly as well.

Web thickness measurements (from medium resolution TEM images) of the gel strands yield results from a diameter of 10 nm for the SCC, SCEC and the ACN gel up to 16 nm for the freeze dried gel (Supplementary Fig. 1). The xerogel from acetone turned out so dense, that no web thickness can be determined for single gel strands. Generally, the drying method ideally should not attack the gel network itself but only affect the solvent removal, therefore no difference in web thickness should be expected. However, there might be an influence of tert-butanol in restructuring of the gel network for the freeze-dried gels. This was observed for the solvent exchange to water, which was attempted in this work as well. The hydroxide gels are dissolving in a pure aqueous system, leaving behind a colloidal solution. As an amphoteric compound, indium hydroxide is strongly dominated by pH chemistry being soluble in strong acidic and basic regimes and stable under

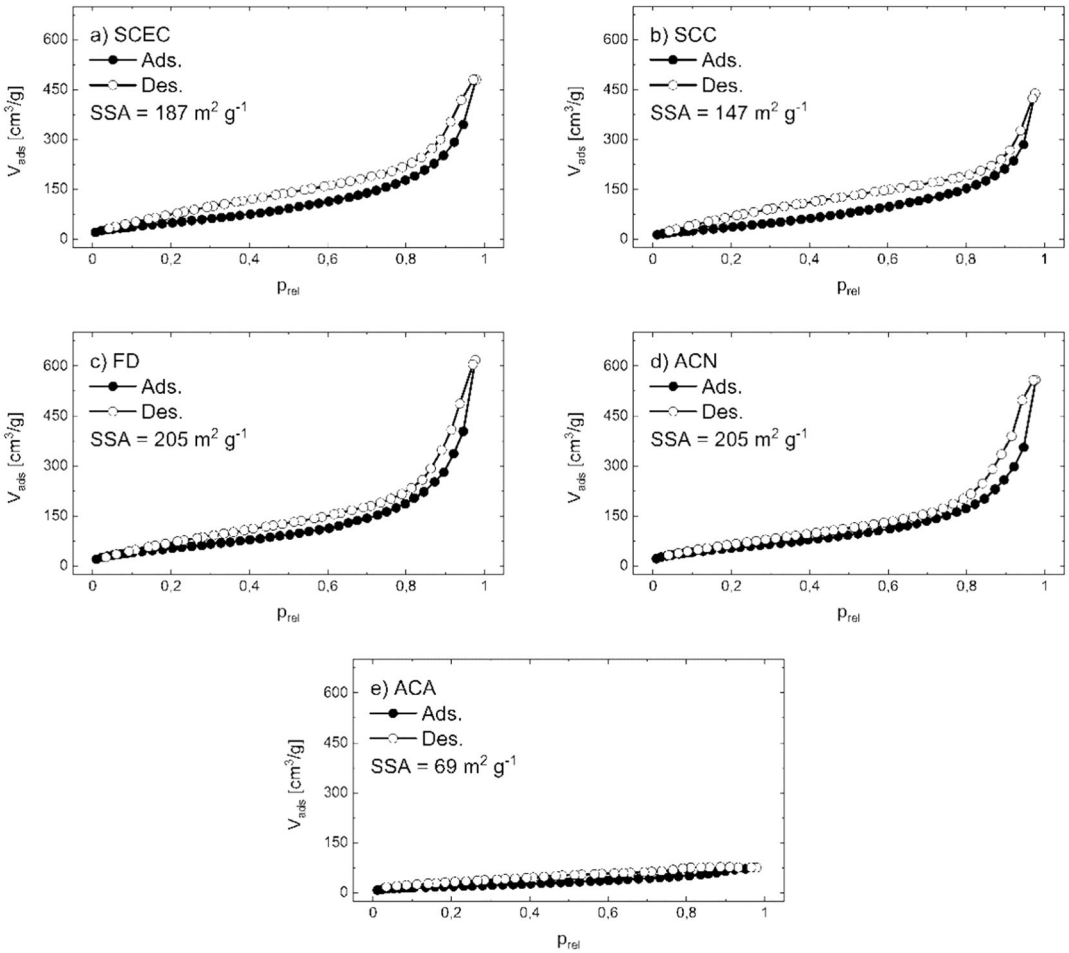

Fig. 4 Adsorption isotherms for gels produced by the (**a**) SCEC, (**b**) SCC, (**c**) FD, (**d**) CAN and (**e**) ACA drying techniques, including specific surface areas (SSA) values

Table 2 Comparison of specific surface area, total pore volume, web thickness and isotherm types for each drying technique

Drying process	SCC	SCEC	FD	ACA	ACN
Specific Surface Area	147 $m^2\ g^{-1}$	187 $m^2\ g^{-1}$	205 $m^2\ g^{-1}$	69 $m^2\ g^{-1}$	205 $m^2\ g^{-1}$
Total pore volume	0,68 $cm^3\ g^{-1}$	0,74 $cm^3\ g^{-1}$	0,96 $cm^3\ g^{-1}$	0,11 $cm^3\ g^{-1}$	0,86 $cm^3\ g^{-1}$
Web thickness	11 nm	11 nm	16 nm	n/a	9 nm
Isotherm type	II	II	II	Undefined	II

neutral conditions. Not controlling the pH in the purely aqueous solution at all, does not lead to a complete dissolution of the gel network, but the reversal of the interconnecting particles forming the gel network reforming a colloidal solution. Another reasoning for the change in web thickness is the formation of small ice crystals which form inside the gel network. It is suspected that these lead to unification of two or more gel strands and consequently bigger web thickness as well as the introduction of large pores, visible in the pore size distribution.

Although showing varying degrees in the amount of adsorbed nitrogen, the gels are not differing much from each other regarding their sorption isotherm type. The adsorption isotherms are shown in Fig. 4, an overview of the gel parameters can be found in Table 2 .The adsorption is characterized by a sharp uptake of nitrogen, which decreases as one monolayer is formed. At high relative pressures the uptake rises again when the pores are filled. The desorption is characteristically defined by a hysteresis, which occurs through the condensation of nitrogen in the pores and finally the isotherms meet back at low relative pressures. Usually for strictly mesoporous systems, the desorption branch meets the adsorption isotherm at a relative pressure of 0,42. The largest specific surface areas could be measured for the gels dried by ACN, SCEC and FD. The BET parameters of the linearized BET

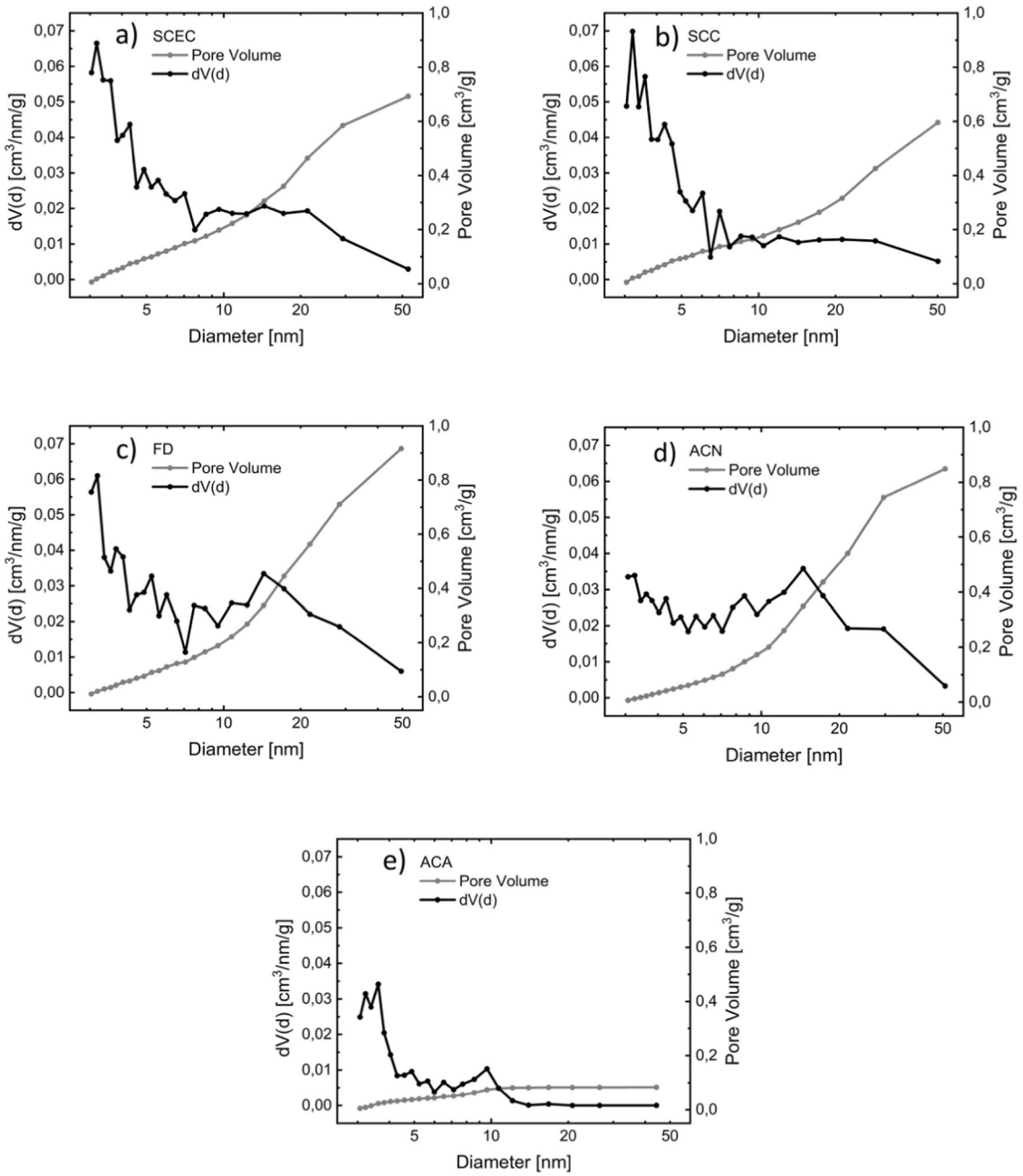

Fig. 5 Pore-size distributions of the five compared gels dried by (**a**) SCEC, (**b**) SCC, (**c**) FD, (**d**) CAN and (**e**) ACA, samples mostly vary in cumulative pore volume as well as size ranges of the pores present

equation also confirm that the multi point BET has been determined in a linear range of the BET equation (Supplementary Table 1).

The pore size analyses stem from the desorption branch of the isotherms from high to medium relative pressures (Fig. 5). Since the model of BET analysis for the nitrogen adsorption experiments can only make assumptions on mesopores, we can show the results for the pore size analysis from 2–50 nm diameter pores. The pore size distribution shows similar distributions for the ACN, SCEC and FD technique. It is characterized by a broad distribution of pores, with a steep uptake in Cumulative Pore Volume (CPV) at larger mesopores. Those are more strongly represented in the CPV, as with the same number of larger pores, the CPV will increase more than for the same amount of smaller mesopores. The pore collapse in the ACA technique leads generally to less pores (lower CPV and Total Pore Volume (TPV) as well as increasingly smaller pores. This can be attributed to the shrinking of the gel network, causing a shift to smaller pores. Especially large mesopores

do not contribute at all to the cumulative pore volume anymore for this sample. Micropores can be analyzed at low relative pressure in a region, where our device unfortunately does not resolve the pressure well enough. One indication for the presence of micropores can be a comparatively large uptake on the first measuring point at low relative pressure. However, the generally low uptake at low relative pressure does not hint to the pronounced presence of micropores (Supplementary Table 2).

Macropores are as well not represented in the results of the BET model. For a purely mesoporous system, the nitrogen uptake at high relative pressure should lessen and finally flatten out towards the highest point of measuring. All the pores are then filled and no more nitrogen can be taken up in the gel network. The type II isotherm character of the adsorption isotherms hints towards the presence of macropores. In all of the samples aside from the ACA method, a continuing uptake of nitrogen can be observed leading up to the highest measurement points, meaning that larger pores are still getting filled in this region. This leads to the conclusion that the compared dried gel systems consist mostly of meso- and macropores, with the only exception being the ACA method. Here, at high relative pressure there can be observed less of an uptake in nitrogen. For this drying process the pore collapse seems to affect the macropores as well.

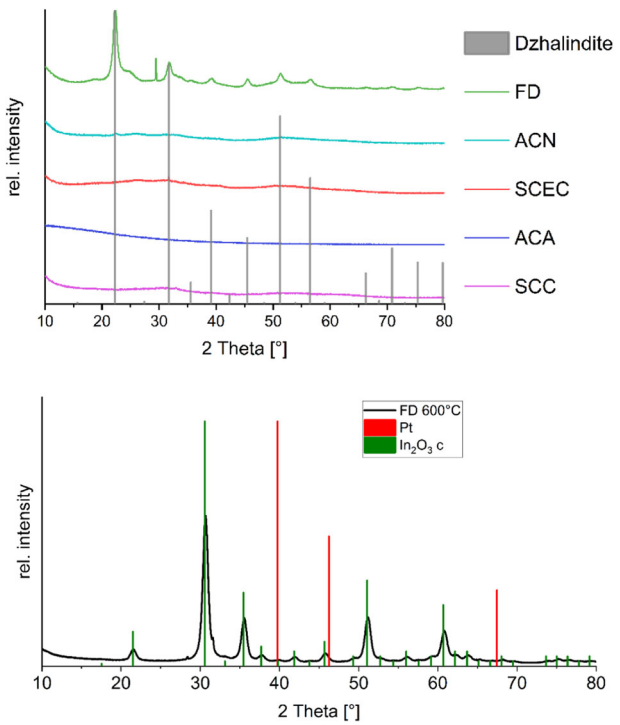

Fig. 6 Top: XRD results of the untreated samples after drying. Only the FD method shows signals in XRD hinting to a crystallization of the gels either due to attack on the gel network by tert-Butanol solvent exchange or a crystallization process at lower temperatures. Bottom: XRD of the FD sample heated at 2 h at 600 °C shows the formation of cubic indium oxide reflexes. Broad reflexes hint at the still small crystallite size of indium oxide, while reflexes of Platinum particles are overlapped by those of indium oxide

The TPV indicates analogous trends to the specific surface areas (Table 2). The value stems from the measuring point at the highest relative pressure, where it is supposed that all pores should be filled with nitrogen. The lowest pore volume can be attributed to the ACA method, explainable by the strong shrinkage of the gel as well of the pore collapse. The slight shrinkage of the ACN method gel however does not lead to a lower TPV. This can be explained by the fact, that the pores are mostly still intact and are not lost even under ambient conditions drying.

The samples show mostly an amorphous signal in powder-XRD measurements, characterized by a decrease in scattering intensity from small to larger scattering angles (Fig. 6). In most publications about this gelation method, gels in this stage are often referred to as metal oxide gels. This claim cannot be proven by XRD measurements. In the presence of water, required for the hydrolysis of the epoxide, the formation of hydroxides is far more likely. Purely oxidic gels can in literature then only be obtained by calcination of the dried gels and the expulsion of water to form the oxides [20, 21]. The freeze dried sample shows reflexes of indium hydroxide (dzhalindite). The presence of reflexes after freeze drying can possibly be explained by crystallization processes of the amorphous hydroxide under the strongly cooled drying conditions. The morphology of the FD sample also shows a more polygonal structuring of the gel branches, compared to the other used methods. For this sample it can be seen in the TEM pictures as well, that there are disconnected particles besides the main gel network located on the TEM grid. Based on their size it is likely that these are platinum particles, affected by the freeze-drying procedure and disconnected from the rest of the network. A dissolution caused by tert-butanol should be visible by the naked eye, as the excess solvent during solvent exchange should turn black after the gels have soaked in it. This is one impact of drying the samples under more extreme conditions, than needed for the other drying techniques. Reflexes of platinum do not show up in the powder diffractogramms as the particles are in the range of only few nm and the expected broadened reflexes are lost in the background scattering of the amorphous signal. Full characterization of the activation of the aerogels for catalysis including calcination for the formation of pure indium oxide, the reduction leading to the formation of intermetallic phases on the aerogel network as well as high resolution TEM imaging of the gels at those stages can be found in our previous work [9].

Thermogravimetric measurements (Fig. 7) up to 300 °C lead to the formation of an indium oxide phase. Full characterization of the oxidative and reductive

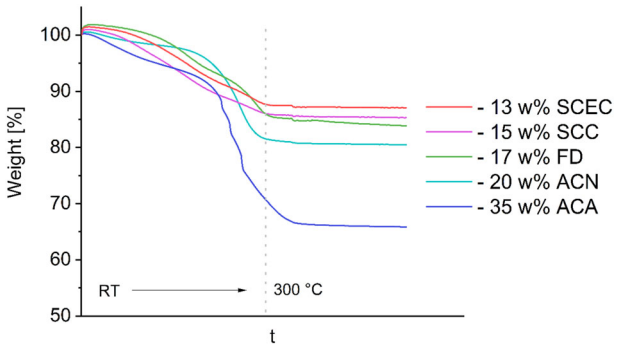

Fig. 7 Thermogravimetric results of heating the gels up to 300 °C and keeping the temperature for an hour. Theoretical weight loss is 16 w% which fits the results for the majority of samples. The ACA sample shows a higher weight loss, due to more solvent trapped in the pores when drying

treatment can be found in our previous publication [9]. This is accompanied by a mass loss of 13% to 20% for most samples and 35 wt% for the ACA gel. Assuming the calcination starts with pure indium hydroxide ($MW = 165\ g\ mol^{-1}$) and ends with pure indium oxide ($MW = 277\ g\ mol^{-1}$) a theoretical weight loss of 16% is expected (with two units of indium hydroxide forming one unit of indium oxide)

$$\frac{(165,84 * 2) - 277,64}{(165,84 * 2)} = 0,1629 \approx 16,3\,w\%$$

The drying technique SCEC, applying the highest temperature during drying, yields the lowest mass loss during temperature treatment hinting to a partly expulsion of water during the drying of the gels at the higher temperatures during the drying process. The largest mass loss can be attributed to the ACA method. During drying at ambient conditions acetone is probably trapped in the pores and can only leave the system under application of higher temperatures over a long period of time.

4 Conclusion

The drying techniques and resulting aerogels cannot directly give indications towards the later performance of the aerogels in catalysis. Still, it is an important energy consuming step in gel synthesis and a possible adaptation of this new material in industrial applications. It can be considered energy consuming as energy needed to remove the solvent leaves the system with the solvent and cannot be recovered easily, in contrast to the gelation process or the solvent exchange which happen in closed systems. The largest specific surface areas and total pore volumes can be reached with either supercritical-, freeze- or ambient conditions drying using NOVEC 7000 as the solvent. The latter exhibits a low surface tension and boiling point reducing the capillary forces of the solvent during evaporation. The biggest impact on morphology can be seen for the FD samples, affecting the crystallinity as well as the platinum loading. The ACA samples experience a complete collapse of the pore system and end up as compact blocks due to capillary forces of acetone on the gel matrix during drying. Finally, the impact of fluorinated solvents shall be discussed here shortly. Fluorinated or chlorinated hydrocarbons usually inhibit a longevity in the environment as they usually cannot be disintegrated by organisms in nature. Past experiences have already proven also the risk of those reaching the atmosphere and causing the depletion of the ozone layer [22]. Although these new generation solvents are sold as environmentally friendly, long-term studies on this are not available to the authors` best knowledge and large-scale use must be advised with caution. Possible might be the use in a circulatory system, where the solvent will be recaptured from the solvent mix during solvent exchange and the evaporating solvent in the drying process. As a proven method, supercritical drying yields consistent results although it seems, that a suitable solvent choice for ambient conditions drying can pose a technologically less intensive and more easily scalable alternative.

Author contributions All authors contributed to the study conception and design. Material preparation, data collection and analysis were performed by NM and LT. The first draft of the manuscript was written by LT and all authors commented on previous versions of the manuscript. All authors read and approved the final manuscript.

Funding The author wishes to express his gratitude towards the Deutsche Bundesstiftung Umwelt for funding this project by a PhD scholarship. Also, we acknowledge the Leibniz-Institut für Polymerforschung Dresden e.V. for access to the TEM facility. Open Access funding enabled and organized by Projekt DEAL.

Compliance with ethical standards

Conflict of interest The authors declare no competing interests.

Publisher's note Springer Nature remains neutral with regard to jurisdictional claims in published maps and institutional affiliations.

References

1. Kistler SS (1931) Coherent expanded aerogels. Nature 127:741. https://doi.org/10.5254/1.3539386.
2. Liu W et al. (2015) Noble metal aerogels-synthesis, characterization, and application as electrocatalysts. Acc Chem Res 48(2):154–162. https://doi.org/10.1021/ar500237c.
3. Cai B, Wen D, Liu W, Herrmann AK, Benad A, Eychmüller A (2015) Function-led design of aerogels: self-assembly of alloyed PdNi hollow nanospheres for efficient electrocatalysis. Angew Chem Int Ed 54(44):13101–13105. https://doi.org/10.1002/anie.201505307.
4. Pierre AC, Pajonk GM (2002) Chemistry of aerogels and their applications. Chem Rev 102(11):4243–4266. https://doi.org/10.1021/cr0101306.
5. Zaera F (2013) Nanostructured materials for applications in heterogeneous catalysis. Chem Soc Rev 42(7):2746–2762. https://doi.org/10.1039/c2cs35261c.
6. Ziegler C, Wolf A, Liu W, Herrmann A, Gaponik N, Eychmüller A (2017) Modern inorganic aerogels. Angew Chem Int Ed 56(43):13200–13221. https://doi.org/10.1002/anie.201611552.
7. Gash AE, Tillotson TM, Satcher Jr JH, Hrubesh LW, Simpson RL (2001) New Sol-gel synthetic route to transition and main-group metal oxide aerogels using inorganic salt precursors. J Non Cryst Solids 285(1–3):22–28. https://doi.org/10.1016/S0022-3093(01)00427-6.
8. Vedyagin AA et al. (2017) Sol–gel synthesis and characterization of two-component systems based on MgO. J Sol Gel Sci Technol 82(2):611–619. https://doi.org/10.1007/s10971-017-4321-3.
9. Köwitsch N et al. (2021) Unprecedented catalytic activity and selectivity in methanol steam reforming by reactive transformation of intermetallic In–Pt compounds. J Phys Chem C 125(18 May):9809–9817. https://doi.org/10.1021/acs.jpcc.1c02260.
10. Köwitsch N et al. (2021) Proving a paradigm in methanol steam reforming: catalytically highly selective InxPdy/In2O3Interfaces. ACS Catal, 304–312, https://doi.org/10.1021/acscatal.0c04073.
11. Iswar S, Malfait WJ, Balog S, Winnefeld F, Lattuada M, Koebel MM (2017) Effect of aging on silica aerogel properties. Microporous Mesoporous Mater 241:293–302. https://doi.org/10.1016/j.micromeso.2016.11.037.
12. Sivaraman D, Zhao S, Iswar S, Lattuada M, Malfait WJ (2021) Aerogel spring-back correlates with strain recovery: effect of silica concentration and aging. Adv Eng Mater 23(10):1–12. https://doi.org/10.1002/adem.202100376.
13. Job N et al. (2005) Carbon aerogels, cryogels and xerogels: influence of the drying method on the textural properties of porous carbon materials. Carbon N Y 43(12):2481–2494. https://doi.org/10.1016/J.CARBON.2005.04.031.
14. Ganesan K, Dennstedt A, Barowski A, Ratke L (2016) Design of aerogels, cryogels and xerogels of cellulose with hierarchical porous structures. Mater Des 92:345–355. https://doi.org/10.1016/J.MATDES.2015.12.041.
15. Groult S, Buwalda S, Budtova T (2021) Pectin hydrogels, aerogels, cryogels and xerogels: Influence of drying on structural and release properties. Eur Polym J 149:110386. https://doi.org/10.1016/J.EURPOLYMJ.2021.110386.
16. Tewari PH, Hunt AJ, Lofftus KD (1985) Ambient-temperature supercritical drying of transparent silica aerogels. Mater Lett 3(9–10):363–367. https://doi.org/10.1016/0167-577X(85)90077-1.
17. van Bommel MJ, de Haan AB (1994) Drying of silica gels with supercritical carbon dioxide. J Mater Sci 29(4):943–948. https://doi.org/10.1007/BF00351414.
18. van Bommel MJ, de Haan AB (1995) Drying of silica aerogel with supercritical carbon dioxide. J Non Cryst Solids 186:78–82. https://doi.org/10.1016/0022-3093(95)00072-0.
19. Steiner III SA, Griffin JS, Nelson RT (2021) Aerogel materials and methods for their production. U.S. Patent Application Nr. 17/104,044.
20. Baumann TF, Gash AE, Chinn SC, Sawvel AM, Maxwell RS, Satcher JH (2005) Synthesis of high-surface-area alumina aerogels without the use of alkoxide precursors. Chem Mater 17(2):395–401. https://doi.org/10.1021/cm048800m.
21. Benad A et al. (2018) Mechanical properties of metal oxide aerogels. Chem Mater 30(1):145–152. https://doi.org/10.1021/acs.chemmater.7b03911.
22. Farman JC, Gardiner BG, Shanklin JD (1985) Large losses of total ozone in Antarctica. Nature 315:207–210.